

At the heart of the proton

Egle Tomasi-Gustafsson^{1,*} and Simone Pacetti^{2,**}

¹DPhN, IRFU, CEA, Université Paris-Saclay, 91191 Gif-sur-Yvette Cedex, France

²Dipartimento di Fisica e Geologia, and INFN Sezione di Perugia, 06123 Perugia, Italy

Abstract. Two main findings on electromagnetic hadron form factors focussed a large interest of the hadron physics community in the recent years. One is the decrease of the electric to magnetic form factor ratio when the momentum transfer in electron proton elastic scattering increases. The second is the discovery of regular oscillations of the generalized proton form factors in the annihilation process electron-positron into proton-antiproton. In this talk we propose a coherent interpretation of these findings giving a general, dynamical description of the proton in the space-time frame which is based on the presence of a quantum vacuum at very small distances.

1 Introduction

The internal structure of protons and neutrons, and in general composite particles is conveniently described in terms form factors (FFs) (for a review, see Ref. [1]). The interaction of electrons with protons p and neutrons n that are spin 1/2 particles, occurs in the first approximation through the exchange of one photon that carries a four momentum q . Assuming parity and time-invariance, as well as charge conservation, the interesting vertex $\gamma^* NN$, ($N = n, p$) is parametrized in terms of two electromagnetic FFs, electric G_E and magnetic G_M , functions of q^2 only. This vertex was experimentally investigated through elastic ep scattering particularly at SLAC, JLab, and Mainz. The accessed kinematical region, called spacelike region, corresponds to negative values of q^2 and, in this region, FFs are real functions due to unitarity. The positive region of four momentum transfer square above the kinematical threshold, $q^2 > 4M^2$ (M is the nucleon mass), can be investigated through the annihilation reactions $e^+ + e^- \rightarrow \bar{p} + p$, currently studied at Novosibirsk [2] and BESIII [3, 4], and $\bar{p} + p \rightarrow e^+ + e^-$, planned at the future facility PANDA-FAIR [5]. These reactions are related by time invariance and crossing symmetry, so that analytical properties of FFs can be inferred from one kinematical region to the other. For example, the complex nature of FFs in timelike region is dictated by unitarity but the imaginary part must vanish at large $|q^2|$, due to the Phragmén-Lindelöf theorem.

Two findings recently impulsed large theoretical and experimental work in the field of hadron electromagnetic FFs.

- **In the spacelike region** the possibilities opened by the polarized high-intensity beam of JLab, combined by large angle spectrometers and hadron polarimeters in the GeV region, allowed to apply the recoil proton polarization transfer method, suggested by A.I. Akhiezer

*e-mail: egle.tomasi@cea.fr

**e-mail: simone.pacetti@unipg.it

and M.P. Rekalo [6, 7]. The measurements were not only more precise as expected, but they established a monotone decrease of the electric to magnetic FF ratio, as a function of $Q^2 = -q^2$, earlier assumed to be constant (Fig. 1). The electric and magnetic distributions (related to FFs by Fourier transforms, in the Breit frame as well as in non-relativistic approach) are different and the difference increases as $|q^2|$ increases, i.e., decreasing the length scale probed by the virtual photon. Extrapolating this behavior (attributed only to G_E as G_M is considered well known from unpolarized experiments) it could be that G_E crosses zero and even becomes negative! Further experiments to elucidate this point are planned in the next future [8].

- **In the timelike region** regular oscillations on the top of a monotonically decreasing background were found in a re-analysis of the BABAR data [9, 10], when plotting the generalized FF data as a function of the modulus of the relative three-momentum of the produced nucleons in the laboratory system $p_L = \sqrt{E^2 - M^2}$, where $E = q^2/(2M) + M$ is the total energy [11]. The world data were successfully reproduced with a six-parameter fit based on a background function (a tripole in q^2) and a damped regularly oscillating sinusoidal. These structures were confirmed by BES data, both with initial state radiation (ISR) [4] and beam scan [3] methods. A similar behavior was found for the neutron, see Fig. 2, where the data could be fitted in a partial range by the same function, with parameters differing only by a phase [12].

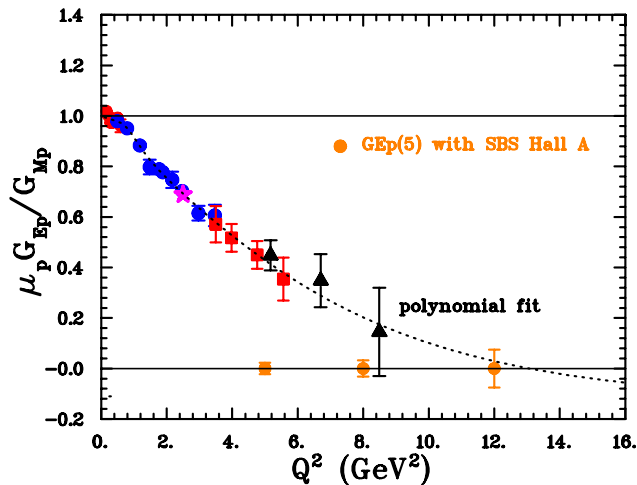


Figure 1. Proton FF ratio from the JLab-GEp Collaboration as a function of $Q^2 = -q^2$. Different symbols correspond to different measurements [13]. Projections of experimental uncertainties for the future JLab experiment E12-07-109 [8] (orange disks) are also shown. The dotted line is a polynomial fit.

In the pioneering [11] and subsequent works [15–17], the oscillating behavior was explained as an interference of two mechanisms, acting at the hadron and at the quark scales, demonstrating the complex dynamical nature of the proton. More recently, different explanations have been put forward [18, 19].

We interpret the data both in spacelike and timelike regions according to the model of Ref. [20], and we assume that at very small distances quarks become colorless due to a region of high intensity chomo-magnetic gluon field [21]. We show that such assumption allows to describe the data, in particular the Q^2 -decreasing behavior of the FF ratio in the spacelike

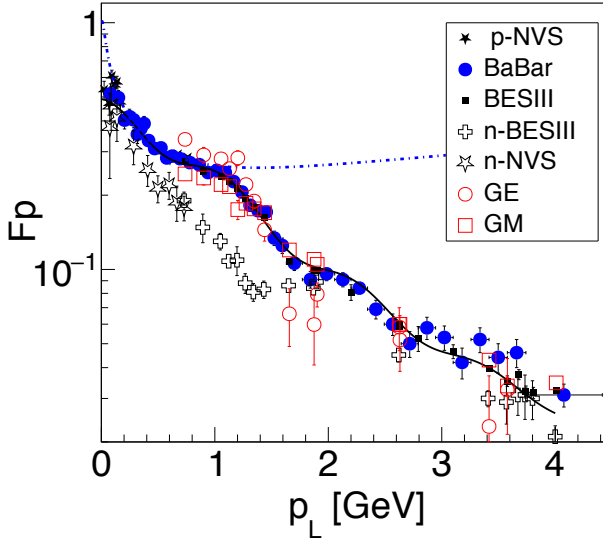


Figure 2. Timelike FF of the nucleon as a function of the relative momentum p_L : generalized FF from the BESIII Collaboration [14] (solid black squares), from the CMD Collaboration [2] (solid black stars) and from the BaBAR Collaboration [9, 10] (solid blue circles); the electric (open red circles) and magnetic FF of the proton (open red squares) are from [14]. The black solid line is the six parameter fit from Ref. [15]. For a pointlike-proton a constant cross section is expected and the corresponding FF is shown as blue dot-dashed line. The neutron FF is shown as open black symbols, from the CMD Collaboration [2] (stars) and from the BESIII Collaboration [12] (crosses).

region, and to predict that no zero crossing will take place. In the timelike region, the model suggests a dynamical description of the proton structure, explaining the astonishing correlation found between hadron generalized FFs. The time and space structure of the proton can be highlighted up to very small scales.

2 Model and data

In the spacelike region, FFs have a clear interpretation in non relativistic approximation, where they are the Fourier transforms of the electric charge and magnetic spatial density distributions. This holds especially in the Breit system, where the energy of the virtual photon is zero, and, similarly to the non-relativistic case, its four-momentum reduces to a three-momentum, $q = (0, \vec{q})$. One can state that in spacelike region FFs contain information on the electric and magnetic distributions of the hadron at a scale defined by the four-momentum of the virtual photon.

In the timelike region, FFs are derived in the center of mass system (CMS), where the three momentum is zero, i.e., $q = (q_0, \vec{0})$. Only the time component of the four momentum transfer is relevant. Therefore, timelike FFs can not bring any spatial information. However, considering the annihilation $e^+ + e^- \rightarrow \bar{p} + p$, FFs keep the memory of the process from the moment of annihilation to the detection, allowing eventually to associate the time scale to the distance of the centers of the forming hadrons.

In order to formalize these concepts in the whole kinematical region, a general definition has been introduced in Ref. [20]. FFs are functions of q^2 only, therefore it is possible to define a relativistic invariant in the following way

$$F(q^2) = \int_{\mathcal{D}} d^4x e^{iq_\mu x^\mu} \rho(x), \quad q_\mu x^\mu = q_0 t - \vec{q} \cdot \vec{x}, \quad (1)$$

where $\rho(x) = \rho(t, \vec{x})$ can be understood as the spacelike distribution of the charge in a space-time volume \mathcal{D} .

In the Breit system the usual definition of spacelike FFs is recovered, while in the annihilation channel, FFs are the Fourier transforms of a function $Q(t)$, that describes the time evolution of the charge distribution in the domain \mathcal{D} . This means that what we measure are the projections of the generalized function on the space and on the time axis, in the Breit system and in CMS, respectively.

The nucleon description in terms of constituent quarks or vector dominance models assumes that the three colored valence quarks are surrounded by a neutral sea of quark-antiquark pairs and gluons. A different picture is suggested by the model of Ref. [20]. The center volume of the nucleon is assumed to be neutral: the strong gluonic field creates a gluon condensate, with a randomly oriented chromo-magnetic field [21]. At very small distances the gluon field as well as the chromo-electric field increases, inducing a screening effect that acts only on the electric FF, leaving the magnetic distribution unchanged, similarly to the Coulomb field in a plasma. The magnetic distribution is expected to follow a Q^2 -dipole dependence, according to the scaling rules of QCD, while the electric distribution is suppressed by an extra factor of $1/Q^2$.

The hadron formation in e^+e^- annihilation can be described through three main steps in terms of evolution in time.

In order to create the hadron-antihadron pair, the energy at the e^+e^- annihilation, concentrated in a small volume, should be at least equal or larger than the threshold energy, $E_{Th} = 2M_h$ (M_h being the hadron and antihadron mass). Then, $q\bar{q}$ pairs are created by the vacuum fluctuations, with the same probability independently on flavor. However, due to the uncertainty principle, the time associated with the $q\bar{q}$ pair depends on their mass and hence on the flavor, the heavier the $q\bar{q}$ pair, the shorter the formation time. This affects the probability to create a hadron-antihadron pair, which requires for the $p\bar{p}$ final channel, that two pairs $u\bar{u}$ and one pair $d\bar{d}$ are created in a space-time volume of dimensions $[\hbar/(2M_h)]^3 \simeq (0.1 \text{ fm})^3$. Below the physical threshold one expects that a system, constituted by at least three bare quark-antiquark pairs, is formed. This system, with the quantum numbers of the photon, can be considered pointlike and colorless, due to the screening of the strong chromo-electromagnetic field.

In the region of strong chromo-electromagnetic field, due to stochastic averaging, the color quantum number does not play any role. Therefore, due to the Pauli principle, quarks of the same flavor, uu for proton and dd for neutron, leave the central region, and one of them is attracted by the remaining quark, d in the proton and u in the neutron, forming a diquark. As the system expands and cools down, the strength of the gluon field decreases and the color degree of freedom is restored. This step is driven by the balance of the electric attraction force and the stochastic force of the gluon field. It is predicted to occur at a distance of 0.2-0.3 fm. The quarks absorb gluons and transform into constituent quarks with mass and magnetic moment. The last step is the formation of the hadron-antihadron pair moving apart, as a results of the competition between the available kinetic energy, $T = \sqrt{q^2} - E_{Th}$ and the confinement energy, $k_s/2R_{pp}$, where $k_s \simeq 1 \text{ GeV/fm}$ is the confinement elasticity constant and R_{pp} is the distance between the centers of the forming hadron and antihadron. When the velocity is very small, a bound state can be formed with dimensions up to hundreds of fm.

2.1 The spacelike region

The suggestion of an electric screening due to the gluon condensate inside the hadron gives a natural explanation of the Q^2 -decrease of the electric FF (Fig. 1) compared to the magnetic one. The data on the proton electric FF, G_E , can be plotted as a function of the wavelength of the virtual photon, i.e., the probed internal distance r which is related to the momentum transfer square q^2 by : r [fm] = $\hbar c / \sqrt{|q^2|} \simeq 0.197$ [GeV fm] / $\sqrt{|q^2|}$ [GeV]. The electric FF, that is not directly measured, is derived from the G_E/G_M ratio assuming G_M known (for example from the fit of Ref. [22]). Data were collected up to very small momentum transfer square (up to 10^{-4} GeV²) in view of determining the proton radius. In Fig. 3 one can see that the resolving power of a photon of such a small four-momentum square is very large, up to 15 fm. Therefore one may wonder how such a photon can give a meaningful information on the proton dimension that is 20 times smaller. This argument supports the quantitative discussion of Refs. [23, 24].

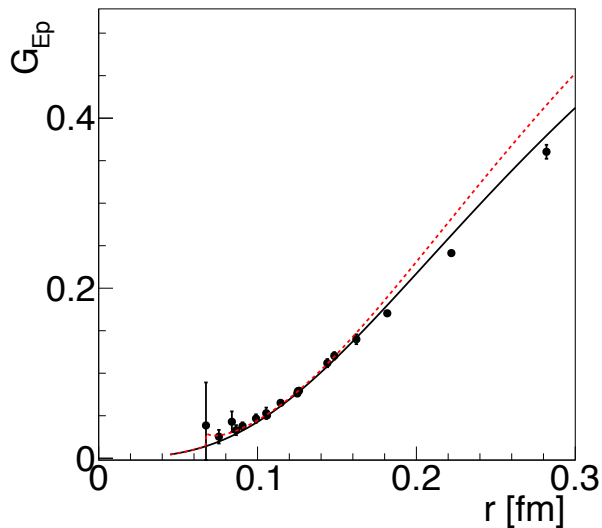


Figure 3. Electric proton FF as a function of the internal distance r seen by the virtual photon. The points are from Ref. [13] and references therein. The dashed red line is a $|q^2|$ -linear fit of the highest $|q^2|$ points, the solid black line corresponds to a Q^2 -monopole fit of the ratio. Figure from Ref. [25].

2.2 The timelike region

The model predicts several features of the timelike FFs data, in particular the interference of quark, diquark and hadron states that may coexist and induce regular oscillations. For a pointlike-proton, a constant cross section $\sigma = 0.87$ mb, corresponding to $|G_E| = |G_M| = 1$, is expected. The corresponding generalized FF is shown as blue dashed line in Fig. 2. One can see that it is compatible with the data in a particular kinematical region.

The three regimes sketched above to follow the evolution of the system, should be observed in the annihilation into a neutron-antineutron pair, as well as hyperon-antihyperon, where one or more light quarks are replaced by strange quarks. Therefore one expects some correlation among these FFs. Let us focus on the generalized FF, as the separation between electric and magnetic FFs is made recently available only for the neutron.

Plotting the effective FF of the neutron versus the proton one measured at the same p_L , Fig. 4, one sees an intriguing behavior. When data are not available at the same p_L , the proton FF has been calculated from the six-parameter proton data fit of Ref. [15] and plotted as black asterisks otherwise as red triangles. The dashed red line corresponds to $F_n = F_p$. Note that the FF threshold values lie at the right top of the figure and those at large q^2 are the points gathered near the origin. Three regimes and two regions are visible, with two breaking points indicated by the thin and thick vertical lines. It is tempting to associate these regimes to the three steps of the evolution of the system sketched above. The large q^2 values, i.e., the shorter times from the annihilation point, correspond to the bottom left of the figure, while the threshold region to the top right. The three pointlike-quark state follows roughly the line $F_n = F_p$, not distinguishing the quark flavor. The step with diquark formation is characterized by the independence of F_n with respect to F_p as the charge is redistributed, and the quark content is not the same here. Near threshold, the quarks dressed by the gluon energy become constituent quarks, following a similar process in neutron and proton, up to the hadron formation.

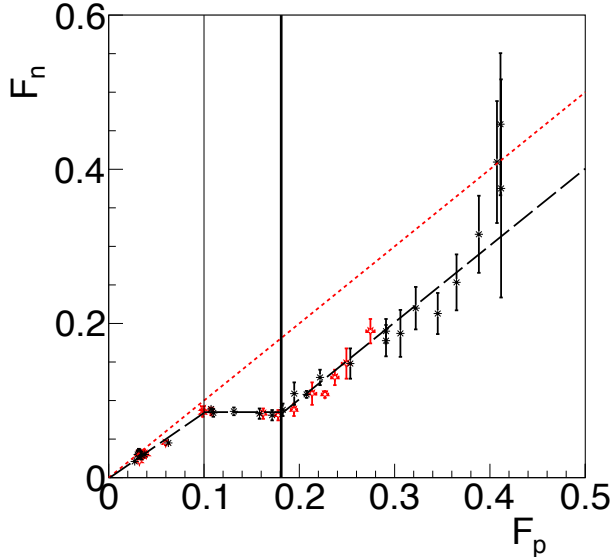


Figure 4. Neutron versus proton effective FF, measured at corresponding p_L (red open stars). When the data are not present at the same p_L , F_p is calculated from the six-parameter fit from Ref. [15] (black asterisks). The red dashed line shows $F_n = F_p$, the black long dashed line is drawn to drive the eyes. The thin and thick black solid lines delimit the region of discontinuity (see text).

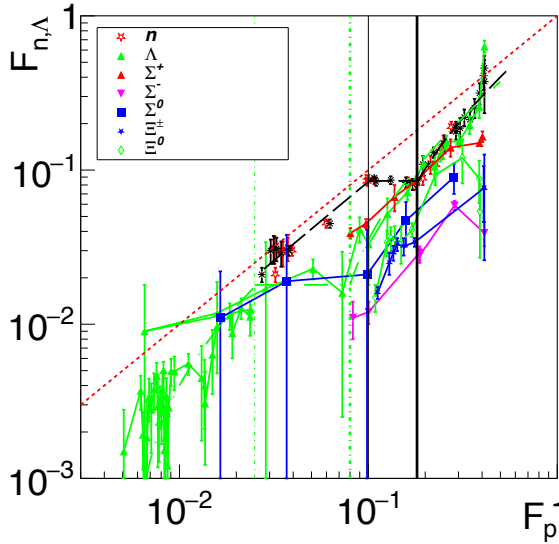


Figure 5. Same as Fig. 4 adding available data on heavier baryons: Λ (green triangles), Σ^+ (red triangles), Σ^- (magenta triangles), Ξ^\pm (blue asterisks), Ξ^0 (open green diamonds).

Similar correlation should be present for heavier baryons, the hyperons where one (or more) light quarks are replaced by heavier strange quarks. Quark pairs are created by quantum vacuum fluctuations: all quark flavors are equally probable, but, due to Heisenberg principle, the associated time, therefore the probability of gathering to create a specific baryon, depends on the energy (the mass of the baryon).

Fig. 5 shows, in addition, available data on heavier baryons. The most extended data concern the reaction $e^+e^- \rightarrow \Lambda + \bar{\Lambda}$. Although not with the same quality as neutrons and protons, they show a very similar behavior. However, the transition among the regimes is somehow shifted towards shorter times. This is expected from the fact that strange quark-antiquark pairs are heavier, corresponding to a shorter time for their production and recombination.

3 Conclusion

We have reviewed hadron FF data in the spacelike and timelike regions, highlighted specific features that are widely discussed in the literature. We have presented a model that gives a coherent description of the scattering and annihilation processes, accounting for the experimental observations.

In particular, the recent data are consistent with the presence of a neutral region in the center volume of the baryon, at very small distances, that is responsible for a steeper Q^2 -decrease of the electric FF compared to the magnetic one. This region can be determined from the elastic scattering data to have a size smaller than 0.06 fm. If it is the case, one can predict that the FF ratio will stay small around zero, at increasing $|q^2|$. This prediction will be soon confirmed or infirmed by the planned experiments at JLab12.

Our model and the present data allow to have an insight of the dynamical structure of the proton for times much smaller than the time for the light to cross the proton, that is 10^{-23} s. One can give a very precise time scale from the annihilation point to the hadron formation in the range: 0.01-0.03 in units of 10^{-23} s. Even more precisely one can situate the transition from the pointlike-quark state to the detectable hadron, through a complex state of different configurations. Among them, there are overlapping configurations, with different probabilities, including diquarks, at the level of $(0.028 - 0.035) \cdot 10^{-23}$ s for nucleons and slightly shorter for strange baryons: $(0.018 - 0.022) \cdot 10^{-23}$ s. This region corresponds to the expansion of the quark and gluon system created from the e^+e^- annihilation to constituent quarks and to the detected hadron.

A similar behavior, but with a different scale between hyperons and nucleons can be understood, as mentioned above, by the different mass of quarks involved. In the instanton picture [21] a classification of the currents and a mass scale for the formation of the different hadrons were suggested, based on the dependence on quantum numbers of the interaction with the vacuum field.

References

- [1] S. Pacetti, R. Baldini Ferroli, E. Tomasi-Gustafsson, Phys. Rept. **550-551**, 1 (2015)
- [2] R.R. Akhmetshin *et al.* (CMD-3 Collaboration), Phys. Lett. **B794**, 64 (2019)
- [3] M. Ablikim *et al.* (BESIII Collaboration), Phys. Rev. Lett. **124**, 042001 (2020)
- [4] M. Ablikim *et al.* (BESIII Collaboration), Phys. Rev. **D99**, 092002 (2019)
- [5] B. Singh *et al.* (PANDA Collaboration), Eur. Phys. J. A **52**, 325 (2016)
- [6] A. Akhiezer, M. Rekalov, Sov. Phys. Dokl. **13**, 572 (1968)
- [7] A. Akhiezer, M. Rekalov, Sov. J. Part. Nucl. **4**, 277 (1974)
- [8] E.J. Brash *et al.* JLab Experiment E12-07-109 (2009)
- [9] J. Lees *et al.* (BaBar Collaboration), Phys. Rev. **D87**, 092005 (2013)
- [10] J. Lees *et al.* (BaBar Collaboration), Phys. Rev. **D88**, 072009 (2013)
- [11] A. Bianconi, E. Tomasi-Gustafsson, Phys. Rev. Lett. **114**, 232301 (2015)
- [12] M. Ablikim *et al.* (BESIII Collaboration), Nature Phys. **17**, 1200 (2021)
- [13] A.J.R. Puckett *et al.* [The GEP Collaboration], Phys. Rev. **C96**, 055203 (2017)
- [14] M. Ablikim *et al.* (BESIII Collaboration), Phys. Rev. Lett. **124**, 042001 (2020)
- [15] E. Tomasi-Gustafsson, A. Bianconi, S. Pacetti, Phys. Rev. C **103**, 035203 (2021)
- [16] A. Bianconi, E. Tomasi-Gustafsson, Phys. Rev. C **95**, 015204 (2017)
- [17] A. Bianconi, E. Tomasi-Gustafsson, Phys. Rev. C **93**, 035201 (2016)
- [18] X. Cao, J.P. Dai, H. Lenske, Phys. Rev. D **105**, L071503 (2022)
- [19] J. Haidenbauer, X.W. Kang, U.G. Meißner, Nucl. Phys. A **929**, 102 (2014)
- [20] E.A. Kuraev, E. Tomasi-Gustafsson, A. Dbeyssi, Phys. Lett. B **712**, 240 (2012)
- [21] A.I. Vainshtein, V.I. Zakharov, V.A. Novikov, M.A. Shifman, Sov. J. Part. Nucl. **13**, 224 (1982)
- [22] E.J. Brash, A. Kozlov, S. Li, G.M. Huber, Physical Review C **65**, 051001(R) (2002)
- [23] S. Pacetti, E. Tomasi-Gustafsson, Eur. Phys. J. A **56**, 74 (2020)
- [24] S. Pacetti, E. Tomasi-Gustafsson, Eur. Phys. J. A **57**, 72 (2021)
- [25] E. Tomasi-Gustafsson, S. Pacetti, Phys. Rev. C **106**, 035203 (2022)